Geophysical Research Letters

RESEARCH LETTER
10.1029/2023GL107451

Enhanced Aerosol Mass in the Tropical Tropopause Layer Linked to Ozone Abundance

Shang Liu[1], Troy D. Thornberry[2], Pengfei Yu[3], Sarah Woods[4], Karen H. Rosenlof[2], and Ru-Shan Gao[2]

[1]Department of Civil and Environmental Engineering, Northeastern University, Boston, MA, USA, [2]NOAA Chemical Sciences Laboratory, Boulder, CO, USA, [3]Institute for Environmental and Climate Research, Jinan University, Guangzhou, China, [4]Earth Observing Laboratory, National Center for Atmospheric Research (NCAR), Boulder, CO, USA

Key Points:

- Aircraft measurements reveal persistent enhancement of aerosol mass in the TTL
- The TTL aerosol enhancement tightly correlates with ozone. An empirical parameterization of TTL aerosol as a function of ozone is derived
- Modeling suggests that TTL aerosol particles are mainly composed of organics and sulfate

Supporting Information:

Supporting Information may be found in the online version of this article.

Correspondence to:

S. Liu and R.-S. Gao,
shang.liu@northeastern.edu;
rushan.gao@noaa.gov

Citation:

Liu, S., Thornberry, T. D., Yu, P., Woods, S., Rosenlof, K. H., & Gao, R.-S. (2024). Enhanced aerosol mass in the tropical tropopause layer linked to ozone abundance. *Geophysical Research Letters*, *51*, e2023GL107451. https://doi.org/10.1029/2023GL107451

Received 21 NOV 2023
Accepted 7 MAR 2024

Abstract Aerosol particles play a critical role in the tropical tropopause layer (TTL) through cloud formation and heterogeneous chemistry, influencing the radiative and chemical balance of the stratosphere. However, aerosol measurements in the TTL are sparse, resulting in poor knowledge of aerosol abundance and distribution in this important region. Here, we present in situ aircraft measurements over the western tropical Pacific, revealing a persistent and altitude-dependent enhancement of aerosol mass in the TTL compared to the convectively influenced troposphere below. Notably, our data demonstrate a striking positive correlation between aerosol mass and ozone. Model simulations suggest that organic materials constitute a substantial fraction of the total aerosol mass within the TTL. We further derived an empirical parameterization of TTL aerosol mass as a function of ozone based on their linear relationship. This framework holds potential for estimating the TTL aerosol abundance but requires further validation and refinement through future measurements.

Plain Language Summary We investigated tiny particles called aerosols in a specific atmospheric layer called the tropical tropopause layer (TTL). These particles are crucial because they affect cloud formation and chemical processes in the atmosphere, influencing how energy is distributed. Unfortunately, there hasn't been much research on aerosols in the TTL, leading to gaps in our understanding of their abundance and distribution in this important region. To fill this knowledge gap, we conducted measurements using aircraft over the western tropical Pacific. Our findings revealed that aerosol mass in the TTL is consistently higher compared to the lower troposphere, which is influenced by upward air movement. What's interesting is that we observed a clear connection between the amount of aerosol and ozone. Our model simulations indicated that a significant portion of the aerosol mass in the TTL is made up of organic materials. To make it easier to estimate aerosol levels and their impact on climate, we developed a way to predict TTL aerosol mass based on ozone measurements. Since ozone is relatively straightforward to measure and model, our method could provide a useful framework for understanding aerosol abundance in the TTL and its effects on the climate.

1. Introduction

As the main pathway for the transport of tropospheric air into the stratosphere, the TTL largely determines the entry values for the materials entering the stratosphere (Fueglistaler et al., 2009). The properties of the TTL air and the processes occurring in the TTL thus affect the global stratosphere and climate (Randel & Jensen, 2013; SPARC, 2006).

Aerosol is an important component in the TTL. The composition of the TTL aerosol is influenced by tropical dynamics (e.g., transport) and regional continental air sources (Froyd et al., 2009). Field observations have suggested that new particle formation events frequently occur in the TTL, in particular the lower TTL just below the tropopause (Brock et al., 1995; Weigel et al., 2011, 2021). Recent advancements in in-situ SO_2 measurement in the TTL suggest little contribution of SO_2 to stratospheric aerosols, revealing a significant gap in the stratospheric aerosol budget (Rollins et al., 2017). Aerosol particles in the TTL affect the stratospheric water vapor budget through TTL dehydration processes by serving as nuclei for the formation of cirrus clouds (Penner et al., 2009). TTL circus clouds have substantial impacts on the earth's radiative balance (Hong et al., 2016). By providing condensed surface areas, TTL aerosol can also facilitate condensation of low vapor pressure gases such as sulfuric acid (Brock et al., 1995) and promote heterogeneous chemistry that depletes

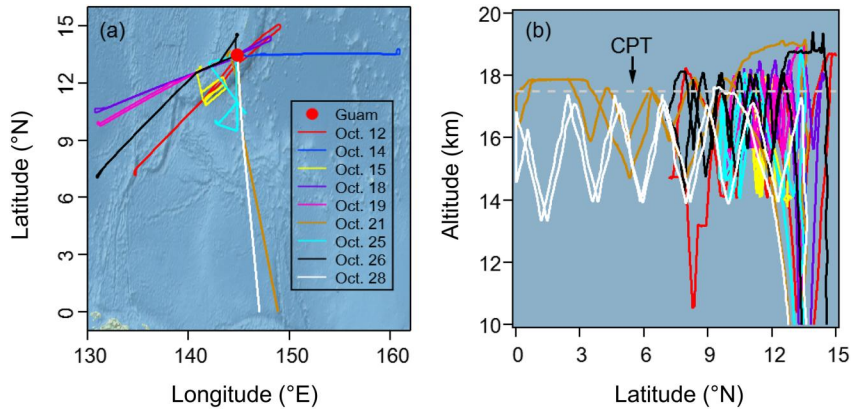

Figure 1. Flight tracks during the POSIDON campaign.

ozone once they are transported to the stratosphere (Tolbert et al., 1988). Despite the importance, the abundance and properties of the TTL aerosol remain poorly characterized. The complex dynamic and chemical processes in the TTL make it difficult to elucidate the formation mechanisms of the TTL aerosol. In-situ measurements of TTL aerosol are limited, hindering our understanding on the climate impacts of the TTL and stratospheric aerosols.

To gain a deeper insight into the abundance, spatial distribution, and formation mechanisms of TTL aerosols, we carried out aircraft measurements of aerosols over the western Pacific warm pool during the Pacific Oxidants, Sulfur, Ice, Dehydration, and cONvection (POSIDON) campaign in October 2016. The western Pacific warm pool plays a leading role for transport of air into the TTL (Fueglistaler et al., 2005). Our measurements were carried out during nine flights aboard a NASA WB-57F high-altitude aircraft stationed in Guam. Throughout these flights, we extensively characterized TTL aerosols and trace gases (flight tracks are shown in Figure 1). To complement the measurements, we employed modeling techniques to obtain insights into the chemical composition of the aerosols. The combined approach of aerosol measurements, tracer analysis, and modeling offers insight into aerosol abundance and formation mechanisms within the TTL.

2. Methods

2.1. Measurements

The POSIDON campaign, took place during October 2016, aimed at improving our understanding of the physical and chemical processes occurring in the TTL. A total of nine flights were carried out on board the NASA WB-57 high altitude aircraft from Guam (13.5° N, 144.8° E). These flights covered the region from 0 to 15°N and from 130 to 160° E (Figure 1a), with vertical coverage spanning 0–19 km (Figure 1b). Each flight path consisted of several upward and downward segments between 14 and 18 km in altitude, providing extensive sampling of the TTL. The measurement region lies over the tropical warm pool, where high sea surface temperatures lead to widespread deep atmospheric convection (Yan et al., 1992).

The aerosol particles were sampled through a near-isokinetic inlet that reduces the ambient sample speed from the aircraft speed of ~90–200 to ~3 m s^{-1} while maintaining ambient aerosol mixing ratios (Jonsson et al., 1995). This inlet has been employed in various aircraft campaigns for aerosol sampling (e.g., Schwarz et al., 2006). Aerosol number size distribution was measured in situ by a custom-built optical particle counter, the portable optical particle spectrometer (POPS), which was mounted in the fuselage bay of the aircraft. The POPS uses a 405 nm laser to count and size individual aerosol particles with diameters from 140 to 3,000 nm (Gao et al., 2016). The scientific application of the POPS has been demonstrated by recent field campaigns (Cui et al., 2018; Liu et al., 2021; Yu et al., 2017). In the POPS instrument, each particle passing across the laser beam produces a pulse by scattering the laser light. The particle number is determined by the number of the pulses. The particle size is calculated from the intensity of the pulse, which was calibrated using a series of differential mobility analyzer (DMA) size-selected dioctyl sebacate (DOS) particles prior to the campaign. The aerosol mass was calculated from the aerosol number and size assuming that the particles are spherical and have a constant density of

1.6 g cm^{-3}. The mass mixing ratio (MMR) of aerosols was determined as the ratio of aerosol mass to the density of ambient air, which was calculated from the measured air pressure and temperature. A lognormal fit to the measured mass size distribution derived from the POPS measurements in the TTL (Figure S1 in Supporting Information S1) suggests that the POPS measurements captured approximately 50% of the total aerosol mass. Laboratory tests suggest that the POPS instrument used during POSIDON can provide reliable measurements under pressures as low as 70 hPa, which corresponds to an altitude of 18.9 km in this study. Therefore the POPS data acquired above 18.9 km are not used in the analysis.

The size distribution of particles with diameter larger than 3 μm was measured with a fast cloud droplet probe (FCDP). The FCDP detects particle forward scattering to determine the number and size of particles (Lance et al., 2010; McFarquhar et al., 2007). We assume that all particles greater than 3 μm are ice crystals as the number of large aerosol particles in the upper troposphere is negligible (Jensen et al., 2013). We found that ice crystals could likely abrade the inlet materials, resulting in artifacts in POPS-measured aerosol size distribution. Such interference has been observed in previous aircraft measurements (Murphy et al., 2004). For this reason, we excluded the POPS data when ice crystals were present from the analysis.

Additional real-time measurements included: (a) ozone mixing ratio obtained using a custom UV spectrophotometer designed for high altitude airborne deployment with high accuracy and precision (Gao et al., 2012), (b) water vapor mixing ratio measured by a two-channel tunable diode laser-based hygrometer, which is capable of accurately measuring low-concentration (below 1 ppm) water vapor in the upper troposphere and lower stratosphere (Thornberry et al., 2015), (c) N_2O mixing ratio was measured by the PAN and other Trace Hydrohalocarbon ExpeRiment (PANTHER) instrument, which uses gas chromatographs with electron capture and mass spectroscopic detection (Elkins et al., 2002; Wofsy, 2011), and (d) ambient air pressure and temperature measured by the Meteorological Measurement System (MMS; Chan et al., 1989; Scott et al., 1990), which also records aircraft position with 1-s time resolution.

2.2. Modeling

We employed the Community Aerosol and Radiation Model for Atmospheres (CARMA), an advanced sectional aerosol model (Toon et al., 1988; Yu et al., 2015). CARMA is coupled with the Community Earth System Model (CESM), allowing for comprehensive analysis of aerosols. The model operates at a spatial resolution of 1.9° × 2.5° and employs a time step of 30 min. The domain extends from 4.74° N to 23.68° N in latitude and from 137.5° E to 162.5° E in longitude. The model incorporates 35 vertical pressure levels, spanning from the Earth's surface up to 200 hPa, and an additional 21 vertical pressure levels from 200 to 2 hPa. Simulations are nudged to meteorology from Modern-Era Retrospective analysis for Research and Applications, Version 2 (MERRA-2; Gelaro et al., 2017).

In our simulations, the emissions of SO_2, volatile organic compounds (VOCs), and primary organic aerosol (POA) are prescribed from the Coupled Model Intercomparison Project Phase (CMIP5) (Lamarque et al., 2010). VOCs, including isoprene, monoterprene, benzene, xylene, and toluene, are tracked in the CESM (Emmons et al., 2010). We simulated secondary organic aerosol (SOA) gas-particle partitioning using a volatility basis set method following Pye et al. (2010).

CARMA tracks two groups of aerosols, with each group containing 20 size bins. The first group consists of pure sulfate particles with aerosol diameter ranging from 0.4 nm to 2.6 μm. These particles form through nucleation and condensation of water and sulfuric acid vapor (Zhao & Turco, 1995). The second group comprises internally mixed aerosols with the diameters varying from 100 nm to 17 μm. These mixed aerosols consist of particles that contain organic compounds, black carbon (BC), sea salt, dust, and condensed sulfate.

In addition, we employed a straightforward, observationally constrained chemical model to characterize the vertical distribution of O_3 within the TTL. This model is a one-dimensional column model that allows updrafts and vertical mixing but assumes no horizontal mixing. The O_3 formation process is represented using the Chapman mechanism (Seinfeld & Pandis, 2016). The model calculation is performed in the aircraft measurement region for the altitude range of 14.5–18.9 km, with an input O_3 concentration of 28.8 ppb at 14.5 km, which represents the average observed O_3 concentration at that altitude. A detailed description of the model is provided in the Supporting Information.

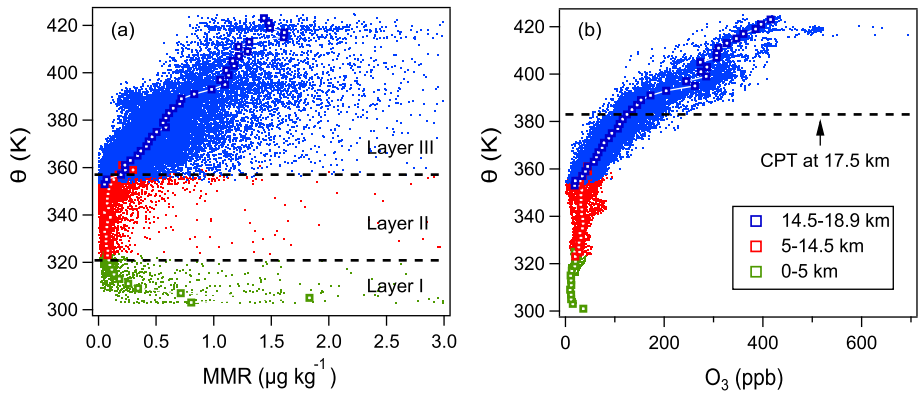

Figure 2. Potential temperature (θ) versus (a) MMR and (b) O_3 for data acquired from 0 to 5, 5–14.5, and 14.5–18.9 km measurements for all flights. Individual data points (5-s averages) are shown by the dots and the averages (by θ of 2 K) are shown by the solid squares.

3. Results and Discussion

3.1. Determination of TTL

We adopt the upper boundary of the TTL to be at 19 km, following SPARC (2006). This altitude is 1.5 km higher than the cold point tropopause (CPT) as shown in Figure S2 in Supporting Information S1. The CPT corresponds to an altitude of 17.5 km and air temperature of approximately 190 K. These values are in line with previous measurements of TTL (Fueglistaler et al., 2009; Gettelman et al., 2004).

The lower boundary of the TTL is determined by examining the vertical profile of potential temperature (θ; Figure S3 in Supporting Information S1). The curvature of the altitude-θ profile changes at 14.5 km, which is mathematically characterized as the lapse rate minimum (LRM) of θ. This change reflects the transition of stability regimes, that is, deep convection dominates air stability below the LRM and radiation starts to influence air temperature above the LRM. Accordingly, we identify the LRM level at 14.5 km (355 K, 140 hPa) as the base of the TTL (Gettelman & Forster, 2002), which is consistent with previous studies (Fueglistaler et al., 2009; Sunilkumar et al., 2017). As a result, the TTL spans from 14.5 to 19 km, and the majority of our measurements were conducted within the TTL (Figure 1).

3.2. Vertical Profile of Aerosols and Ozone

The vertical profile of aerosol mass from the surface to the top of the TTL can be segmented in three layers with distinct characteristics (Figure 2a). Layer I spans from the surface to 5 km altitude and represents the lower troposphere, in which the MMR of aerosols decreased logarithmically with altitude from 2 to 0.08 μg kg^{-1} likely because of the influence of surface emissions from Guam. Layer II ranges from 5 to 14.5 km altitude. In this layer, the aerosol MMR remained at approximately 0.08 μg kg^{-1} with small variability. Such low-concentration aerosol layers immediately below the convection outflow have been observed previously over the Northern Indian Ocean (de Reus et al., 2001) and the rain forests in South America (Andreae et al., 2018; Krejci et al., 2003). The observation indicates that deep convection serves as an effective sink for aerosol particles (Yu et al., 2019). Layer III lies in the TTL, extending from 14.5 to 18.9 km, with the upper boundary 1.4 km higher than the CPT. In this layer the aerosol MMR increased rapidly from 0.08 μg kg^{-1} at 14.5 km to 1.5 μg kg^{-1} at 18.9 km. Our observations show a sustained increase of aerosol MMR from the upper troposphere to lower stratosphere across the tropopause, rather than abrupt transitions. This suggests that the CPT has no unique role for the transport of aerosols. Accounting for the mass of <140 nm particles that were not measured by the POPS instrument, the aerosol MMR at 18.9 km would be approximately 3 μg kg^{-1}. This concentration is close to the measurement during the POLARIS mission in 1997 (Mclinden et al., 1999), in which an aerosol MMR of approximately 3.5 μg kg^{-1} was observed for aerosols with size range of 0.07–1 μm at 18.9 km in eastern Pacific (17.5° N, 159.3° W).

The ozone concentration remained below 35 ppb in layers I and II and began to increase at 14.5 km (Figure 2b). This observation is consistent with previous ozonesonde measurements in the tropical Pacific (Folkins

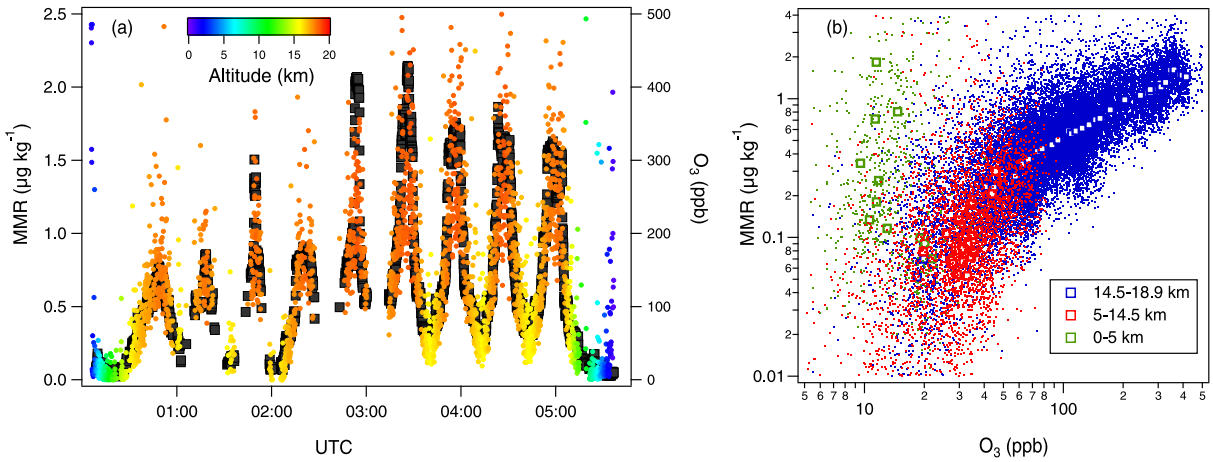

Figure 3. (a) Example time series of aerosol MMR and O_3 for the October 18 measurements. MMR is represented by solid circles and colored by flight altitude. O_3 is represented by solid squares (not colored by altitude change). The gaps indicate ice-influenced data that were excluded from the analysis. (b) Scatter plot of MMR versus O_3 for the 0–5 km (layer I), 5–14.5 km (layer II), and 14.5–18.9 km (layer III) measurements. Individual data points are shown by the dots and the averages are shown by the solid squares. Logarithmic scales are used to make the small values visible.

et al., 1999; Folkins & Martin, 2005). The concurrence of ozone minimum and LRM is in line with the analysis by Gettelman and Forster (2002) and Folkins et al. (2002).

3.3. Mechanisms for Aerosol Enhancement in the TTL

We find that the aerosol MMR was tightly correlated with O_3 in the TTL during all flights with small variation between flights. This can be clearly seen in the example time series of O_3 and aerosol MMR for the flight on October 18 shown in Figure 3a. The Pearson's correlation coefficient (r) for the campaign-average O_3 and aerosol MMR (averaged into 2-K θ intervals) was 0.98 in layer III. In contrast, the aerosol MMR and O_3 were anti-correlated with an r value of −0.35 in layer I (Figure 3b), and no correlation was observed between aerosol MMR and O_3 in layer II.

The main processes contributing to the increase in TTL O_3 from the bottom to the top of the TTL include chemical production via photolytic dissociation of molecular oxygen (O_2) (Crutzen et al., 1999; Prather, 2009) and isentropic in-mixing of stratospheric air from the extratropical lower stratosphere (Konopka et al., 2010; Ploeger et al., 2012). The relative contribution of these processes to O_3 remains unclear. While some studies argue that in situ chemical production dominates (Avallone & Prather, 1996), others suggest that isentropic stratospheric in-mixing can contribute to O_3 by as much as 40%–60% (Abalos, Randel, et al., 2013, Abalos, Randel, et al., 2013; Konopka et al., 2009, 2010; Ploeger et al., 2011, 2012; Sargent et al., 2014). This contribution is most significant during the boreal summer months (June–August), primarily driven by the Asian summer monsoon, and gradually decreases during transition into the fall and winter months. In particular, these studies suggest that the contribution from in-mixing falls within the range of 0%–20% in October, averaged over a ±10°N latitude range, with the contribution increasing with altitude.

We used a one-dimensional column model (over the flight region) and tracer analysis to examine these processes. The model calculates the vertical distribution of O_3 within the TTL, considering a constant slow vertical ascent rate of 0.25 mm s^{-1} (Avallone & Prather, 1996; Park et al., 2010) of air in the TTL and assuming it evolves in isolation (the model description section in the Supporting Information). Remarkably, the calculated vertical profile of O_3 closely aligns with the observed O_3 profile (Figure 4a). This result is in line with earlier investigations that yielded similar results using a column model (Avallone & Prather, 1996) and with research that assumed the tropics are isolated from extra-tropics when explaining the annual cycles of ozone above the tropical tropopause (Randel et al., 2007; Schoeberl et al., 2008). However, we acknowledge the simplicity of the model. For example, the model does not consider the chemistry of nitrogen oxides (NO and NO_2; not measured during POSIDON) and O_3, which could be important in the TTL O_3 abundance (Nussbaumer et al., 2003), and uncertainties exist in the assumed ascent rate. On the other hand, the tracer analysis shows evidence of stratospheric in-mixing. Figure S4 in Supporting Information S1 shows that N_2O was anticorrelated with O_3 in the TTL during

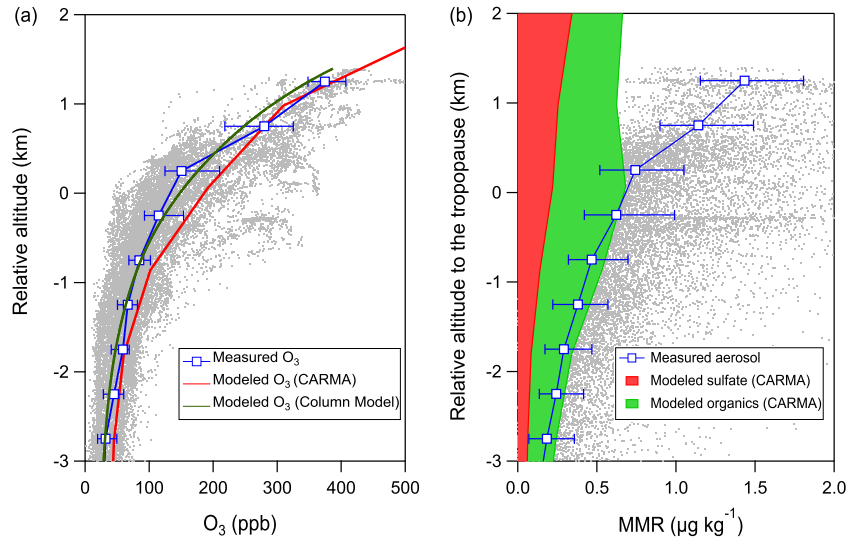

Figure 4. Comparison of modeling results to measurements for (a) O_3 and (b) aerosol MMR. Individual measurement points are shown by the gray dots. The median values and the 25th and 75th percentiles are shown by the blue line-square symbols and the error bars. The *y*-axis represents altitude relative to the tropopause.

POSIDON. The observed negative correlation indicates that the sampled TTL air included a contribution from mixing of stratospheric origin (Folkins et al., 1999). This is because the strong UV radiation at higher altitudes in the stratosphere photolyzes N_2O while leading to O_3 production, resulting in an anticorrelation of N_2O and O_3 (Assonov et al., 2013). In contrast, N_2O in the troposphere is inert and uniformly distributed, thus anticorrelation of N_2O with O_3 is not expected and not observed below the TTL during our measurements. The synthesis of modeling and tracer analysis indicates contributions from both chemical production and stratospheric in-mixing to TTL O_3. Given the strong correlation between O_3 and aerosols in the TTL, these results suggest it is possible that TTL aerosols might also be influenced by these chemical and physical processes.

To investigate the chemical composition of TTL aerosol, we employed the CARMA model embedded in CESM to simulate the aerosol formation and growth processes. The model reproduced the O_3 profile reasonably well (Figure 4a). Our model results suggest that sulfate aerosol exhibits a consistent increase with altitude, whereas organic aerosol displays an ascending trend below the tropopause but declines above it. Simulated contributions of black carbon, dust, and sea salt are negligible partly because these aerosols are removed through the secondary activation above the cloud base via deep convection (Yu et al., 2019). Moreover, our modeled vertical profile of the total aerosol MMR demonstrates good agreement with the in situ measurements (Figure 4b) below the tropopause, with organic aerosol constituting a significant fraction of the aerosol mass. These modeling results imply that sulfur alone is insufficient to explain the observed aerosol mass, and organic precursors may play a pivotal role in the formation and/or growth of TTL aerosols under low-temperature conditions. This finding aligns with previous findings from TTL measurements during the Pre-AVE and CR-AVE campaigns over Southwest Central America in boreal winter (Froyd et al., 2009), which highlighted the prevalence of organic-sulfate particles as the most abundant particle type in the TTL and lower stratosphere. We note that the model underestimates the aerosol mass above the tropopause, with the difference increasing with altitude within the TTL, reaching 60% at an altitude of 1 km above the CPT. Additional research is needed to understand this discrepancy.

We postulate that TTL aerosols are likely generated through the processes of new particle formation and subsequent growth following convective outflow in the upper troposphere (Williamson et al., 2019). The observed aerosol number size distribution in the TTL suggests particle growth with increasing altitude (Figure S5 in Supporting Information S1), although obtaining measurements of smaller particles would enhance our understanding. During convective transport, soluble species are effectively removed, whereas the insoluble and weakly soluble species can endure washout and gradually ascend upward, with minimal loss, to reach the stratosphere (Bechara et al., 2010). The TTL, characterized by low temperature, low particle surface area density, and high

relative humidity, provides ideal conditions for new particle formation and growth. Multiple studies have proposed the upper troposphere as the primary nucleation region (Brock et al., 1995; Weigel et al., 2011), and investigations have revealed the involvement of organics in new particle formation and initial growth in the remote tropical upper troposphere (Kupc et al., 2020). Froyd et al. (2009) observed an increase in the signal of particulate oxidized organics with altitude in the TTL up to 19 km via aircraft measurements. They hypothesized that this increase could be attributed to particle growth through aging processes. Future measurements analyzing the composition of oxidized organic species will enhance our understanding of particle formation and growth pathways. Exceptional overshooting that crosses the tropical tropopause could also affect the aerosol abundance in the TTL (Vernier et al., 2011). This possibility is examined using H_2O as a tracer. The θ-H_2O profile displayed no spikes above the tropopause (Figure S6 in Supporting Information S1), suggesting the absence of overshooting during the measurements.

Building upon the strong correlation between TTL aerosol mass and O_3 in our measurements, we further derived an empirical parameterization of aerosol MMR as a function of O_3 in the TTL using linear regression. The derived relationship is expressed as MMR ($\mu g\ kg^{-1}$) = 0.0074 ($\pm 2.2 \times 10^{-4}$) × O_3 (ppb) + 0.23 ($\pm$0.049), accounting for the 50% mass that was not measured by the POPS instrument. This parameterization may be used to estimate TTL aerosol abundance and for validation of modeled results within the measurement region during the measurement months.

4. Conclusions

Our aircraft measurements conducted over the western Pacific revealed a vertically stratified aerosol distribution comprised of three distinct layers. The lower-troposphere layer, ranging from 0 to 5 km in altitude, exhibited a decrease in aerosol mass with height, primarily influenced by surface-level emissions. The layer between 5 and 14.5 km displayed consistently low aerosol concentrations with minimal variability, indicating effective aerosol removal through deep convection processes. In the TTL, we observed an enhanced aerosol mass that exhibited a strong correlation with O_3. The modeling and tracer analysis suggest that TTL O_3 and aerosols likely originate from a combination of chemical production and stratospheric in-mixing processes. Furthermore, based on the linear relationship observed between aerosol MMR and O_3 in the TTL, we derived an empirical parameterization that may allow for the estimation of aerosol MMR as a function of O_3 within the observation region and during the observation months.

While the parameterization shows promise for estimating TTL aerosol abundance using ozone, which is relatively easier to measure and model, its application is constrained by significant limitations as measurements were conducted in a specific region of the TTL under background conditions during a particular time period, and the POPS instrument had limited measurement capabilities, including assumptions about aerosol density and a limited particle measurement range that excludes smaller particles. Therefore this framework requires extensive future research for verification and improvement.

Our study also highlights the challenge of accurately predicting aerosol mass, particularly above the tropopause, even for the most advanced models. This underscores the existence of significant gaps in our understanding of the origin and formation mechanisms of aerosols in the TTL. To achieve a more comprehensive understanding of TTL aerosol, it is crucial to conduct future measurements that encompass detailed aerosol chemical composition and gas-phase precursors across different locations and seasons. These endeavors will help diagnose potential deficiencies in the models and validate the modeling results. Consequently, they will lead to an improved comprehension of TTL aerosols and facilitate a predictive understanding of their effects on stratospheric chemistry, clouds, and climate.

Data Availability Statement

The aircraft measurements during the POSIDON field campaign are available through the NASA ESPO Data Archive: https://espoarchive.nasa.gov/archive/browse/posidon/WB57.

Acknowledgments
We appreciate the funding support from ERB. We would like to thank Paul Lawson from APEC Incorporated for the help with collecting the FCDP data. We are also thankful to Paul Bui for providing the MMS data.

References

Abalos, M., Ploeger, F., Konopka, P., Randel, W. J., & Serrano, E. (2013). Ozone seasonality above the tropical tropopause: Reconciling the Eulerian and Lagrangian perspectives of transport processes. *Atmospheric Chemistry and Physics*, *13*(21), 10787–10794. https://doi.org/10.5194/acp-13-10787-2013

Abalos, M., Randel, W. J., Kinnison, D. E., & Serrano, E. (2013). Quantifying tracer transport in the tropical lower stratosphere using WACCM. *Atmospheric Chemistry and Physics*, *13*(21), 10591–10607. https://doi.org/10.5194/acp-13-10591-2013

Andreae, M. O., Afchine, A., Albrecht, R., Holanda, B. A., Artaxo, P., Barbosa, H. M. J., et al. (2018). Aerosol characteristics and particle production in the upper troposphere over the Amazon Basin. *Atmospheric Measurement Techniques*, *18*(2), 921–961. https://doi.org/10.5194/acp-18-921-2018

Assonov, S. S., Brenninkmeijer, C. A. M., Schuck, T., & Umezawa, T. (2013). N_2O as a tracer of mixing stratospheric and tropospheric air based on CARIBIC data with applications for CO_2. *Atmospheric Environment*, *79*, 769–779. https://doi.org/10.1016/j.atmosenv.2013.07.035

Avallone, L. M., & Prather, M. J. (1996). Photochemical evolution of ozone in the lower tropical stratosphere. *Journal of Geophysical Research*, *101*(D1), 1457–1461. https://doi.org/10.1029/95JD03010

Bechara, J., Borbon, A., Jambert, C., Colomb, A., & Perros, P. E. (2010). Evidence of the impact of deep convection on reactive volatile organic compounds in the upper tropical troposphere during the AMMA experiment in West Africa. *Atmospheric Chemistry and Physics*, *10*(21), 10321–10334. https://doi.org/10.5194/acp-10-10321-2010

Brock, C. A., Hamill, P., Wilson, J. C., Jonsson, H. H., & Chan, K. R. (1995). Particle formation in the upper tropical troposphere: A source of nuclei for the stratospheric aerosol. *Science*, *270*(5242), 1650–1653. https://doi.org/10.1126/science.270.5242.1650

Chan, K. R., Scott, S. G., Bui, T. P., Bowen, S. W., & Day, J. (1989). Temperature and horizontal wind measurements on the ER-2 aircraft during the 1987 airborne Antarctic ozone experiment. *Journal of Geophysical Research*, *94*(D9), 11573–11587. https://doi.org/10.1029/JD094iD09p11573

Crutzen, P. J., Lawrence, M. G., & Poschl, U. (1999). On the background photochemistry of tropospheric ozone. *Tellus*, *51A-B*(1), 123–146. https://doi.org/10.1034/j.1600-0889.1999.00010.x

Cui, Y. Y., Liu, S., Bai, Z., Bian, J., Li, D., Fan, K., et al. (2018). Religious burning as a potential major source of atmospheric fine aerosols in summertime Lhasa on the Tibetan Plateau. *Atmospheric Environment*, *181*, 186–191. https://doi.org/10.1016/j.atmosenv.2018.03.025

de Reus, M., Krejci, R., Williams, J., Fischer, H., Scheele, R., & Strom, J. (2001). Vertical and horizontal distributions of the aerosol number concentration and size distribution over the northern Indian Ocean. *Journal of Geophysical Research*, *106*(D22), 629–641. https://doi.org/10.1029/2001JD900017

Elkins, J. W., Moore, F. L., & Kline, E. S. (2002). Update: New airborne gas chromatograph for NASA airborne platforms. *Proc. Earth Sci. Technol. Conf.*, 1–3.

Emmons, L. K., Walters, S., Hess, P. G., Lamarque, J. F., Pfister, G. G., Fillmore, D., et al. (2010). Description and evaluation of the model for ozone and related chemical tracers, version 4 (MOZART-4), Geosci. *Model Dev*, *3*(1), 43–67. https://doi.org/10.5194/gmd-3-43-2010

Folkins, I., Braun, C., Thompson, A. M., & Witte, J. (2002). Tropical ozone as an indicator of deep convection. *Journal of Geophysical Research*, *107*(13), 1–10. https://doi.org/10.1029/2001JD001178

Folkins, I., Loewenstein, M., Podolske, J., & Oltmans, J. (1999). A barrier to vertical mixing at 14 km in the tropics: Evidence from ozonesondes and aircraft measurements. *Journal of Geophysical Research*, *104*, 22095–22102. https://doi.org/10.1029/1999JD900404

Folkins, I., & Martin, R. V. (2005). The vertical structure of tropical convection and its impact on the budgets of water vapor and ozone. *Journal of the Atmospheric Sciences*, *62*(5), 1560–1573. https://doi.org/10.1175/jas3407.1

Froyd, K. D., Murphy, D. M., Sanford, T. J., Thomson, D. S., Wilson, J. C., Pfister, L., & Lait, L. (2009). Aerosol composition of the tropical upper troposphere. *Atmospheric Chemistry and Physics*, *9*(13), 4363–4385. https://doi.org/10.5194/acp-9-4363-2009

Fueglistaler, S., Bonazzola, M., Haynes, P. H., & Peter, T. (2005). Stratospheric water vapor predicted from the Lagrangian temperature history of air entering the stratosphere in the tropics. *Journal of Geophysical Research*, *110*, D08107. https://doi.org/10.1029/2004JD005516

Fueglistaler, S., Dessler, A. E., Dunkerton, T. J., Folkins, I., Fu, Q., & Mote, P. W. (2009). Tropical tropopause layer. *Reviews of Geophysics*, *47*(1). https://doi.org/10.1029/2008RG000267

Gao, R. S., Ballard, J., Watts, L. A., Thornberry, T. D., Ciciora, S. J., McLaughlin, R. J., & Fahey, D. W. (2012). A compact, fast UV photometer for measurement of ozone from research aircraft. *Atmospheric Measurement Techniques*, *5*(9), 2201–2210. https://doi.org/10.5194/amt-5-2201-2012

Gao, R. S., Telg, H., McLaughlin, R. J., Ciciora, S. J., Watts, L. A., Richardson, M. S., et al. (2016). A light-weight, high-sensitivity particle spectrometer for $PM_{2.5}$ aerosol measurements. *Aerosol Science & Technology*, *50*(1), 88–99. https://doi.org/10.1080/02786826.2015.1131809

Gelaro, R., McCarty, W., Suarez, M. J., Todling, R., Molod, A., Takacs, L., et al. (2017). The Modern-Era Retrospective analysis for research and applications, version 2 (MERRA-2). *Journal of Climate*, *30*(14), 5419–5454. https://doi.org/10.1175/jcli-d-16-0758.1

Gettelman, A., & Forster, P. M. d. F. (2002). A climatology of the tropical tropopause layer. *J. Meteorol. Soc. Japan*, *80*(4B), 911–924. https://doi.org/10.2151/jmsj.80.911

Gettelman, A., Forster, P. M. D. F., Fujiwara, M., Fu, Q., Vömel, H., Gohar, L. K., et al. (2004). Radiation balance of the tropical tropopause layer. *J. Geophys. Res. Radiation balance of the tropical tropopause layer*, *109*(D7). https://doi.org/10.1029/2003JD004190

Hong, Y., Liu, G., & Li, J.-L. F. (2016). Assessing the radiative effects of global ice clouds based on CloudSat and CALIPSO measurements. *Journal of Climate*, *29*(21), 7651–7674. https://doi.org/10.1175/JCLI-D-15-0799.1

Jensen, E. J., Diskin, G., Lawson, R. P., Lance, S., Bui, T. P., Hlavka, D., et al. (2013). Ice nucleation and dehydration in the tropical tropopause layer. *Proceedings of the National Academy of Sciences*, *110*(6), 2041–2046. https://doi.org/10.1073/pnas.1217104110

Jonsson, H. H., Wilson, J. C., Brock, C. A., Knollenberg, R. G., Newton, R., Dye, J. E., et al. (1995). Performance of a focused cavity aerosol spectrometer for measurements in the stratosphere of particle size in the 0.06-2.0-µm-dimaeter range. *Journal of Atmospheric and Oceanic Technology*, *12*(1), 115–129. https://doi.org/10.1175/1520-0426(1995)012<0115:poafca>2.0.co;2

Konopka, P., Grooß, J.-U., Günther, G., Ploeger, F., Pommrich, R., Müller, R., & Livesey, N. (2010). Annual cycle of ozone at and above thetropical tropopause: Observations versus simulations with the ChemicalLagrangian Model of the Stratosphere (CLaMS). *Atmospheric Chemistry and Physics*, *10*(1), 121–132. https://doi.org/10.5194/acp-10-121-2010

Konopka, P., Grooß, J.-U., Ploeger, F., & Müller, R. (2009). Annual cycleof horizontal in-mixing into the lower tropical stratosphere. *Journal of Geophysical Research*, *114*(D19), D19111. https://doi.org/10.1029/2009JD011955

Krejci, R., Stro, J., Reus, M. D., Hoor, P., Williams, J., Fischer, H., & Hansson, H. (2003). Evolution of aerosol properties over the rain forest in Surinam, South America, observed from aircraft during the LBA-CLAIRE 98 experiment. *Journal of Geophysical Research*, *108*(D18), 1–17. https://doi.org/10.1029/2001JD001375

Kupc, A., Williamson, C. J., Hodshire, A. L., Kazil, J., Ray, E., Bui, T. P., et al. (2020). The potential role of organics in new particle formation and initial growth in the remote tropical upper troposphere. *Atmospheric Chemistry and Physics*, *20*(23), 15037–15060. https://doi.org/10.5194/acp-20-15037-2020

Lamarque, J. F., Bond, T. C., Eyring, V., Granier, C., Heil, A., Klimont, Z., et al. (2010). Historical (1850–2000) gridded anthropogenic and biomass burning emissions of reactive gases and aerosols: Methodology and application. *Atmospheric Chemistry and Physics*, *10*(15), 7017–7039. https://doi.org/10.5194/acp-10-7017-2010

Lance, S., Brock, C. A., Rogers, D., Gordon, J. A., & Oceanic, N. (2010). Water droplet calibration of the Cloud Droplet Probe (CDP) and in-flight performance in liquid, ice and mixed-phase clouds during ARCPAC. *Atmospheric Measurement Techniques*, *3*(6), 1683–1706. https://doi.org/10.5194/amt-3-1683-2010

Liu, S., Liu, C. C., Froyd, K. D., Schill, G. P., Murphy, D. M., Bui, T. P., et al. (2021). Sea spray aerosol concentration modulated by sea surface temperature. *Proceedings of the National Academy of Sciences*, *118*(9). https://doi.org/10.1073/pnas.2020583118

Mcfarquhar, G. M., Um, J., Freer, M., Baumgardner, D., Kok, G. L., & Mace, G. (2007). Importance of small ice crystals to cirrus properties: Observations from the tropical warm pool international cloud experiment. *Geophysical Research Letters*, *34*(13), 1–6. https://doi.org/10.1029/2007GL029865

Mclinden, C. A., McConnell, J. C., McElroy, C. T., & Griffioen, E. (1999). Observations of stratospheric aerosol using CPFM polarized limb radiances. *Journal of the Atmospheric Sciences*, *56*(2), 233–240. https://doi.org/10.1175/1520-0469(1999)056<0233:oosauc>2.0.co;2

Murphy, D. M., Cziczo, D. J., Hudson, P. K., Thomson, D. S., Wilson, J. C., Buseck, P. R., et al. (2004). Particle generation and resuspension in aircraft inlets when flying in clouds particle generation and resuspension in aircraft inlets when flying in clouds. *Aerosol Science & Technology*, *38*(4), 401–409. https://doi.org/10.1080/02786820490443094

Nussbaumer, C. M., Fischer, H., Lelieveld, J., & Pozzer, A. (2003). What controls ozone sensitivity in the upper tropical troposphere? *Atmospheric Chemistry and Physics*, *23*(19), 12651–12669. https://doi.org/10.5194/acp-23-12651-2023

Park, S., Atlas, E. L., Jimenez, R., Daube, B. C., Gottlieb, E. W., Nan, J., et al. (2010). Vertical transport rates and concentrations of OH and Cl radicals in the tropical tropopause layer from observations of CO2 and halocarbons: Implications for distributions of long- and short-lived chemical species. *Atmospheric Chemistry and Physics*, *10*(14), 6669–6684. https://doi.org/10.5194/acp-10-6669-2010

Penner, J. E., Chen, Y., Wang, M., & Liu, X. (2009). Possible influence of anthropogenic aerosols on cirrus clouds and anthropogenic forcing. *Atmospheric Chemistry and Physics*, *9*(3), 879–896. https://doi.org/10.5194/acp-9-879-2009

Ploeger, F., fueglistaler, S., Grooß, J.-U., Günther, G., Konopka, P., Liu, Y. S., et al. (2011). Insight from ozone and water vapour on transportin the tropical tropopause layer (TTL). *Atmospheric Chemistry and Physics*, *11*(1), 407–419. https://doi.org/10.5194/acp-11-407-2011

Ploeger, F., Konopka, P., Müller, R., Fueglistaler, S., Schmidt, T., Manners, J. C., et al. (2012). Horizontal transport affecting trace gas seasonality in the Tropical Tropopause Layer (TTL). *Journal of Geophysical Research*, *117*(D9), D09303. https://doi.org/10.1029/2011JD017267

Prather, M. J. (2009). Tropospheric O_3 from photolysis of O_2. *Geophysical Research Letters*, *36*(3). https://doi.org/10.1029/2008GL036851

Pye, H. O. T., Chan, A. W. H., Barkley, M. P., & Seinfeld, J. H. (2010). Global modeling of organic aerosol: The importance of reactive nitrogen (NO_x and NO_3). *Atmospheric Chemistry and Physics*, *10*, 11261–11276. https://doi.org/10.5194/acp-10-11261-2010

Randel, W. J., & Jensen, E. J. (2013). Physical processes in the tropical tropopause layer and their roles in a changing climate. *Nature Geoscience*, *6*, 169–176. https://doi.org/10.1038/ngeo1733

Randel, W. J., Park, M., Wu, F., & Livesey, N. (2007). A large annual cycle in ozone above the tropical tropopause linked to the Brewer-Dobson circulation. *Journal of the Atmospheric Sciences*, *64*(12), 4479–4488. https://doi.org/10.1175/2007jas2409.1

Rollins, A. W., Thornberry, T. D., Watts, L. A., Yu, P., Rosenlof, K. H., Mills, M., et al. (2017). The role of sulfur dioxide in stratospheric aerosol formation evaluated by using in situ measurements in the tropical lower stratosphere. *Geophysical Research Letters*, *44*(9), 4280–4286. https://doi.org/10.1002/2017GL072754

Sargent, M. R., Smith, J. B., Sayres, D. S., & Anderson, J. G. (2014). The roles of deep convection and extratropical mixing in the tropical tropopause layer: An in situ measurement perspective. *J. Geophys. Res.-Atmos*, *119*(21), 12355–12371. https://doi.org/10.1002/2014JD022157

Schoeberl, M. R., Douglass, A. R., Newman, P. A., Lait, L. R., Lary, D., Waters, J., et al. (2008). QBO and annual cycle variations in tropical lower stratosphere trace gases from HALOE and Aura MLS observations. *Journal of Geophysical Research*, *113*(D5), D05301. https://doi.org/10.1029/2007JD008678

Schwarz, J. P., Gao, R. S., Fahey, D. W., Thomson, D. S., Watts, L. A., Wilson, J. C., et al., (2006). Single-particle measurements of midlatitude black carbon and light-scattering aerosols from the boundary layer to the lower stratosphere. *Journal of Geophysical Research*, *111*(D16). https://doi.org/10.1029/2006JD007076

Scott, S. G., Bui, P. T., Chan, R. K., & Bowen, S. W. (1990). The meteorological measurement system on the NASA ER-2 aircraft. *Journal of Atmospheric and Oceanic Technology*, *7*(4), 525–540. https://doi.org/10.1175/1520-0426(1990)007<0525:tmmsot>2.0.co;2

Seinfeld, J., & Pandis, S. (2016). *Atmospheric chemistry and physics: From air pollution to climate change*. Wiley.

Stratosphere-troposphere Processes and their Role in Climate (2006). Assessment of stratospheric aerosol properties (ASAP), WCRP-124, WMO/TD No. 1295. *SPARC Rep*, *4*.

Sunilkumar, S. V., Muhsin, M., Venkat Ratnam, M., Parameswaran, K., Krishna Murthy, B. V., & Emmanuel, M. (2017). Boundaries of tropical tropopause layer (TTL): A new perspective based on thermal and stability profiles. *Journal of Geophysical Research*, *122*(2), 741–754. https://doi.org/10.1002/2016JD025217

Thornberry, T. D., Rollins, A. W., Gao, R. S., Watts, L. A., Ciciora, S. J., McLaughlin, R. J., & Fahey, D. W. (2015). A two-channel, tunable diode laser-based hygrometer for measurement of water vapor and cirrus cloud ice water content in the upper troposphere and lower stratosphere. *Atmospheric Measurement Techniques*, *8*(1), 211–224. https://doi.org/10.5194/amt-8-211-2015

Tolbert, A., Rossi, J. M., & Golden, D. M. (1988). Heterogeneous interactions of chlorine nitrate, hydrogen chloride, and nitric acid with sulfuric acid surfaces at stratospheric temperatures. *Geophysical Research Letters*, *15*(8), 847–850. https://doi.org/10.1029/GL015i008p00847

Toon, O. B., Turco, R. P., Westphal, D., Malone, R., & Liu, M. (1988). A multidimensional model for aerosols——Description of computational analogs. *Journal of the Atmospheric Sciences*, *45*(15), 2123–2144. https://doi.org/10.1175/1520-0469(1988)045<2123:ammfad>2.0.co;2

Vernier, J., Pommereau, J., Thomason, L. W., Pelon, J., Garnier, A., Deshler, T., et al. (2011). Overshooting of clean tropospheric air in the tropical lower stratosphere as seen by the CALIPSO lidar. *Atmospheric Chemistry and Physics*, *11*(18), 9683–9696. https://doi.org/10.5194/acp-11-9683-2011

Weigel, R., Borrmann, S., Kazil, J., Minikin, A., Stohl, A., Wilson, J. C., et al. (2011). In situ observations of new particle formation in the tropical upper troposphere: The role of clouds and the nucleation mechanism. *Atmospheric Chemistry and Physics*, *11*(18), 9983–10010. https://doi.org/10.5194/acp-11-9983-2011

Weigel, R., Mahnke, C., Baumgartner, M., Dragoneas, A., Vogel, B., Ploeger, F., et al. (2021). In situ observation of new particle formation (NPF) in the tropical tropopause layer of the 2017 Asian monsoon anticyclone – Part 1:Summary of StratoClim results. *Atmospheric Chemistry and Physics*, *21*(15), 11689–11722. https://doi.org/10.5194/acp-21-11689-2021

Williamson, C. J., Kupc, A., Axisa, D., Bilsback, K. R., Bui, T., Campuzano-jost, P., et al. (2019). A large source of cloud condensation nuclei from new particle formation in the tropics. *Nature*, *574*(7778), 399–403. https://doi.org/10.1038/s41586-019-1638-9

Wofsy, S. C. (2011). HIAPER Pole-to-Pole observations (HIPPO): Fine-grained, global-scale measurements of climatically important atmospheric. *Phil. Trans. Roy. Soc. A*, *369*(1943), 2073–2086. https://doi.org/10.1098/rsta.2010.0313

Yan, X., Ho, C., Zheng, Q., & Klemas, V. (1992). Temperature and size variabilities of the western pacific warm pool. *Science*, *258*(5088), 1643–1645. https://doi.org/10.1126/science.258.5088.1643

Yu, P., Froyd, K. D., Portmann, R. W., Toon, O. B., Freitas, S. R., Bardeen, C. G., et al. (2019). Efficient in-cloud removal of aerosols by deep convection. *Geophysical Research Letters*, *46*(2), 1061–1069. https://doi.org/10.1029/2018GL080544

Yu, P., Rosenlof, K. H., Liu, S., Telg, H., Thornberry, T. D., Rollins, A. W., et al. (2017). Efficient transport of tropospheric aerosol into the stratosphere via the Asian summer monsoon anticyclone. *Proceedings of the National Academy of Sciences*, *114*(27), 6972–6977. https://doi.org/10.1073/pnas.1701170114

Yu, P., Toon, O. B., Bardeen, C. G., Mills, M. J., Fan, T., English, J. M., & Neely, R. R. (2015). Evaluations of tropospheric aerosol properties simulated by the community Earth system model with a sectional aerosol microphysics scheme. *Journal of Advances in Modeling Earth Systems*, *7*(2), 865–914. https://doi.org/10.1002/2014ms000421

Zhao, J., & Turco, R. P. (1995). Nucleation simulations in the wake of a jet aircraft in stratospheric flight. *Journal of Aerosol Science*, *26*(5), 779–795. https://doi.org/10.1016/0021-8502(95)00010-a